Published in final edited form as:

Exp Eye Res. 2016 August ; 149: 59–65. doi:10.1016/j.exer.2016.06.015.

Spatial distributions of phosphorylated membrane proteins aquaporin 0 and MP20 across young and aged human lenses

Danielle B. Gutierrez[a,1], **Donita L. Garland**[b,2], **John H. Schwacke**[c,3], **David L. Hachey**[d], and **Kevin L. Schey**[d,*]

[a]Department of Cell and Molecular Pharmacology and Experimental Therapeutics, Medical University of South Carolina, BSB 358 MSC 509, 173 Ashley Ave., Charleston, SC 29425, USA

[b]National Eye Institute, National Institutes of Health, Bethesda, MD 20892, USA

[c]Department of Biostatistics and Epidemiology, Medical University of South Carolina, Cannon Place 303C, 135 Cannon St., Charleston, SC 29425, USA

[d]Mass Spectrometry Research Center, Vanderbilt University School of Medicine, Suite 9160 MRBIII, 465 21st Ave. So., Nashville, TN 37240-7916, USA

Abstract

In the human ocular lens it is now realized that post-translational modifications can alter protein function and/or localization in fiber cells that no longer synthesize proteins. The specific sites of post-translational modification to the abundant ocular lens membrane proteins AQP0 and MP20 have been previously identified and their functional effects are emerging. To further understand how changes in protein function and/or localization induced by these modifications alter lens homeostasis, it is necessary to determine the spatial distributions of these modifications across the lens. In this study, a quantitative LC-MS approach was used to determine the spatial distributions of phosphorylated AQP0 and MP20 peptides from manually dissected, concentric layers of fiber cells from young and aged human lenses. The absolute amounts of phosphorylation were determined for AQP0 Ser235 and Ser229 and for MP20 Ser170 in fiber cells from the lens periphery to the lens center. Phosphorylation of AQP0 Ser229 represented a minor portion of the total phosphorylated AQP0. Changes in spatial distributions of phosphorylated APQ0 Ser235 and MP20 Ser170 correlated with regions of physiological interest in aged lenses, specifically, where barriers to water transport and extracellular diffusion form.

Keywords

Aquaporin 0; Phosphorylation; Mass spectrometry; Membrane protein; MP20; Ocular lens

[*]Corresponding author: k.schey@vanderbilt.edu (K.L. Schey).

[1]Current address: Mass Spectrometry Research Center, Vanderbilt University School of Medicine, PMB 407916, Nashville, TN 37240-7916, USA.

[2]Current address: Department of Ophthalmology, Massachusetts Eye and Ear Infirmary and Harvard Medical School, Boston, MA, USA.

[3]Current address: Scientific Research Corporation, North Charleston, South Carolina, USA.

1. Introduction

At a certain distance from the lens periphery, fiber cells lose their organelles (Bassnett, 2002) and can no longer synthesize new proteins (Faulkner-Jones et al., 2003). As a means of maintaining lens function and transparency, post-translational modifications (PTMs) can alter protein function in a regional manner (Gonen et al., 2004a; Grey et al., 2009; Lin et al., 1998). In order to understand how the effects of PTMs on protein function influence overall lens homeostasis, it is important to determine the spatial distributions of modified proteins across the lens.

Aquaporin 0 (AQP0) and MP20 (also known as LIM2) are two highly modified abundant membrane proteins in lens fiber cells, together constituting over 60% of the membrane protein content (Broekhuyse et al., 1976; Louis et al., 1989). AQP0 functions as a water channel (Chandy et al., 1997; Varadaraj et al., 2005, 1999), an adhesion protein (Gonen et al., 2004a, 2004b; Kumari et al., 2011), and as a structural protein (Al-Ghoul et al., 2003; Lindsey Rose et al., 2006; Shiels et al., 2000), and these functions may be regionally distinct (Ball et al., 2004; Gonen et al., 2004a; Grey et al., 2009). MP20 may play a role in cell adhesion and syncytium formation (Grey et al., 2003; Shiels et al., 2007). Both AQP0 and MP20 are known to be phosphorylated (Ball et al., 2004; Ervin et al., 2005; Louis et al., 1985; Schey et al., 2000); however the spatial distribution of phosphorylated forms and the effects of phosphorylation on APQ0 function are not completely understood.

AQP0 is phosphorylated at Ser229 (pSer229), Ser231 (pSer231), and Ser235 (pSer235) (Ball et al., 2004; Schey et al., 2000) in an AKAP2/PKA regulated process (Gold et al., 2012), and a recent lens membrane proteome analysis identified several additional AQP0 phosphorylation sites (Wang et al., 2013). Phosphorylated AQP0 C-terminal peptides showed decreased affinity for Ca^{2+}-calmodulin (Ca^{2+}-CaM) compared to unmodified C-terminal peptides (Gold et al., 2012; Reichow and Gonen, 2008; Rose et al., 2008). At the intact protein level, AQP0 S229D showed reduced affinity for calmodulin compared to wild type AQP0 (Kalman et al., 2008). Furthermore, the S229D mutant resulted in an AQP0 with high water permeability compared to wild type AQP0 (Kalman et al., 2008). Recently, a mechanism was depicted wherein two Ca^{2+}-CaM molecules bind an AQP0 tetramer, resulting in closure of constriction site II by conserved residues and preventing water permeation through AQP0 (Reichow et al., 2013). Additionally, phosphorylation at Ser235 may be important for AQP0 trafficking to the membrane (Golestaneh et al., 2008) as reported for other aquaporins. For example, AQP2 regulation in the kidney is dependent on trafficking of pAQP2 (Wilson et al., 2013); however, there is no published evidence for AQP0 shuttling in lens fiber cells. This type of energy intensive regulation of protein trafficking may be unlikely in the lens given its limited energy budget. The abundance of AQP0 pSer235 has been measured as highest in the inner cortical region of a 34 yr lens (Ball et al., 2004), and Ca^{2+} increases from 300 nM in the lens cortex to 700 nM in the core (Gao et al., 2004). Therefore, regulation of AQP0 permeability may be dependent on regional differences in Ca^{2+} and pSer235 levels.

Regional changes in AQP0 water permeability are likely to affect lens homeostasis, as predicted by the lens internal circulation system (Mathias et al., 2007, 1997). At around 50

years of age, in a region 6–8 mm from the lens center, a barrier forms that prevents water transport into the lens core (Moffat et al., 1999). It is possible that a decrease in AQP0 water permeability in this region could contribute to the formation of a barrier; however, the phosphorylation state of AQP0 in this region of aged lenses is unknown. Determining the spatial distribution of AQP0 pSer235 will reveal the location within the lens where phosphorylation peaks and the changes that occur with age, thereby enhancing our understanding of AQP0 water permeability regulation throughout the lens.

MP20 is phosphorylated at Ser170 (pSer170) and Thr171 (pThr171) (Ervin et al., 2005); however, the functional effect of MP20 phosphorylation remains to be determined. In the rat lens, MP20 insertion into the fiber cell membrane correlates with the formation of a barrier to extracellular transport (Donaldson et al., 2004; Grey et al., 2003). Recently, a similar barrier was detected in a 69 year old human lens at a normalized lens distance (r/a) of approximately 0.91 where (a) represents the lens radius and (r) represents the distance from the lens core to the region of interest (Lim et al., 2009). It is not known whether MP20 plays a role in the diffusion barrier that forms in aged human lenses, but it is possible that a change in the phosphorylation state of MP20 contributes to its barrier formation.

The aim of this work was to map the distributions and to quantitate the extent of AQP0 and MP20 phosphorylation. This was achieved in both young and aged lenses by careful dissection of lens regions followed by quantitation using AQUA isotopically labeled peptide internal standards and targeted LC-MS/MS. The results demonstrate that the distributions of AQP0 and MP20 phosphorylation change across the lens with age and correlate with regions of physiological interest.

2. Methods

2.1. Lens dissection and tissue preparation

Human lenses of various ages (16, 18, 19, 23, 51, 54, and 60 years) were dissected into 5–7 regions based on developmental fiber cell age (Garland et al., 1996). To compare the location of dissected regions from different lenses, the midpoint distance of each region from the lens center (r) was determined and normalized as a function of the lens radius (a), to yield normalized lens distance (r/ a), where 1.0 represents the lens periphery and 0.0 the lens center (Jacobs et al., 2004). For example, a region dissected from the lens periphery (7.5–8 mm) of an 8 mm diameter lens, has a midpoint radial distance (r) of 7.75 mm, and a normalized lens distance (r/ a = 7.75 mm/8 mm) of 0.97.

Pairs of lenses, young and aged, were homogenized and washed in parallel for the enrichment of membrane proteins, in a manner similar to that described previously (Ball et al., 2004). Membrane protein pellets were suspended in 180 μL of 50 mM NH_4HCO_3, and 20 μL of acetonitrile (MeCN). Trypsin (1–2 μg) was added and the samples were digested for 24 h at 37 °C. After digestion, samples were spun at 16,000 × g at 4 °C for 10 min. To assure that equal amounts of digested lens protein were loaded in each experiment, BCA protein assays of the digested samples were carried out using digested, bovine serum albumin (BSA) as a standard.

2.2. AQUA peptides

AQUA phosphopeptides (Gerber et al., 2003) were synthesized by Sigma Aldrich, with an isotopically labeled arginine ($^{13}C_6$ $^{15}N_4$, Table 1). Each peptide was reconstituted in 10% formic acid (FA) and diluted to 5 pmol/μL (4–6 ng/μL) with 0.1% FA. Individual AQUA peptides were mixed, and this mixture, which included 3.7 ng of AQP0 pSer235 AQUA peptide, 1.4 ng of AQP0 pSer231 AQUA peptide, and 1.2 ng of MP20 pSer170 AQUA peptide, was combined with approximately 420 ng aliquots of lens protein. Spiked lens samples were dried down and stored at −20 °C.

2.3. Mass spectrometry

Prior to injection, samples were solubilized in 50 μL of 0.1% FA. All samples were analyzed on a Thermo Scientific LTQ XL Orbitrap mass spectrometer in line with an Eksigent nanoLC 2D HPLC pump. Samples (approximately 42 ng) were loaded onto a C_{18}, 100 μm id, 6 cm trap column in 98% mobile phase A (100% H_2O, 0.1% FA) and 2% mobile phase B (100% MeCN, 0.1% FA) for 10 min, separated on a C_{18}, 100 μm id, 20 cm analytical column over a 23 min gradient from 2 to 25% mobile phase B, and ionized by nanospray ionization. Mass spectrometry analysis occurred in two stages – identification and quantitation. For identification, MS scans (mass-to-charge ratio (m/ z) 250–1200) were performed in the Orbitrap followed by collision-induced dissociation (CID) of selected ions and MS/MS acquisition in the ion trap. For quantitation, MS scans were carried out in the ion trap. Ions of m/z 275–475 were detected from 0 to 25 min, and ions of m/z 350–800 were detected from 25 to 35 min.

2.4. Data analysis and quantitation

2.4.1. Quantitation of AQUA internal standard and endogenous phosphopeptides—Mass spectra were analyzed using XCalibur Qual Browser version 2.0.7 (Thermo Fisher Scientific), and the area under the curve (AUC) was determined from extracted ion chromatograms (XIC) of endogenous (END) and AQUA internal standard (IS) phosphopeptides. A standard curve was produced from the analysis of AQUA phosphopeptides at various concentrations. These data were fit to a straight line using nonlinear regression in GraphPad Prism 5 Demo. The standard curve for each peptide is shown in Supplemental Fig. 1. The absolute quantity (AQ) of phosphorylation for specific sites on AQP0 and MP20 was determined using Equation (1) below (Brönstrup, 2004; Gerber et al., 2003) and mapped as a function of normalized lens distance for young (n = 3) and aged (n = 3) lenses.

$$\mathrm{AQ}_{\mathrm{END}} = (\mathrm{AUC}_{\mathrm{END}} / \mathrm{AUC}_{\mathrm{IS}}) * \mathrm{AQ}_{\mathrm{IS}} \quad 1$$

2.4.2. Curve fitting—Curve fitting was employed to estimate a continuous distribution of site specific phosphorylation for APQ0 and MP20 in young and aged lenses, using GraphPad Prism 6. As shown in Equation (2) below, a model was chosen that fit the Log distribution of the absolute amounts of phosphorylation. The model expresses the increase in the amount of a product (in this case phosphorylated peptide) from the initial substance and

the subsequent decrease in this product, either to the initial substance or a degradation product,

$$\mathrm{Log\,(Abs.Amt.)}=(\mathrm{A+B-C})*\mathrm{e}^{(-\mathrm{k}_1(1-\mathrm{r}))}-\mathrm{Ae}^{(-\mathrm{k}_2(1-\mathrm{r}))}+\mathrm{C} \quad 2$$

where Abs. Amt. is the mean absolute amount of phosphorylation per sample determined from three replicate injections, r is the normalized lens distance, k_1 and k_2 are rate constants of growth and decay respectively, and A, B, C are constants that describe, respectively, the amplitude scale factor, the minimum value at r = 1, and the plateau of the curve as (r) approaches 0. Values for B were determined for each age group and were shared among the three young lenses. Values for A, C, k_1, and k_2 were determined for each individual lens.

Curves were plotted across a normalized lens distance range of 0.99–0.22 and 0.97–0.11 for young and aged lenses respectively based on the most peripheral and most central normalized lens distances of the dissected lens samples. The maximum amounts of phosphorylation determined from the fitted curves for the young (n = 3) and aged lenses (n = 3) were averaged to determine a mean maximum amount for each age group. The corresponding radial distances (r) for each maximum value were also averaged to determine the mean radial distance at which phosphorylation peaks. Significant differences ($p < 0.05$) in the amounts of phosphorylation between the young and aged lenses at values of r and differences in the amounts of phosphorylation between the pre-and post-permeability barrier regions were determined via a two-way ANOVA repeated measures followed by the Sidak multiple comparisons test.

3. Results

3.1. Identification of phosphopeptides

The present work describes the spatial distributions of phosphorylated AQP0 and MP20 in young and aged lenses. As a first step, the phosphopeptides of interest were identified by their measured molecular weights and MS/MS fragmentation patterns. An example is shown for MP20 pSer170 (Fig. 1). Extracted ion chromatograms (XIC) of endogenous MP20 pSer170 and its respective AQUA phosphopeptide internal standard (Fig. 1, insets) show that the phosphopeptides have equivalent retention times and were distinguishable by a mass difference produced by the isotopic label (10 Da), corresponding to 5 m/z units for the $[M+2H]^{2+}$ ions. Similar data are presented for the APQ0 pSer235 and pSer229 phosphopeptides in Supplemental Figs. 2 and 3. Throughout all runs, retention times were very reproducible so that the phosphopeptides of interest could be identified by their retention time and measured m/z. After identification, absolute quantitation of phosphorylated AQP0 and MP20 was performed via LC-MS analysis.

3.2. Quantitation of MP20 phosphorylation

Absolute quantitation of MP20 pSer170 in dissected lens regions revealed its distribution across the lens. Fig. 2 and Supplemental Fig. 4a show that in young lenses (18–23 years), phosphorylation was highest at an average normalized lens distance of 0.90 (range = 0.85–

0.94). At this distance, the average absolute amount of pSer170 was 4.1 fg (range = 2.8–5.6 fg) per pg of lens membrane protein. In aged lenses (51–60 years), phosphorylation was highest at an average normalized lens distance of 0.91 (range = 0.91–0.92), as seen in Fig. 2 and Supplemental Fig. 4a. At this distance, the average amount of pSer170 was 3.0 fg (range = 2.6–3.5 fg) per pg of lens membrane protein. Although the maximum amount of pSer170 was not significantly different between young and old lenses at this location, the amount of pSer170 was significantly greater in the young lenses compared to the aged lenses beginning at a normalized lens distance of 0.81 (indicated by the dotted vertical line in Fig. 2) and remaining so through to the lens core (Fig. 2 and Supplemental Fig. 4a). In fact, the amount of pSer170, after peaking, remained fairly constant across lens regions in young lenses.

3.3. Quantitation of AQP0 phosphorylation

Previous work has shown that Ser235 is the prominent site of phosphorylation in human AQP0 (Ball et al., 2004). Here, absolute quantitation of AQP0 pSer235 in dissected lens regions revealed its distribution across young and old human lenses. Fig. 3 and Supplemental Fig. 4b show that in young lenses, the amount of pSer235 peaked at an average normalized lens distance of 0.82 (range = 0.78–0.87), where there was an average of 466 fg (range = 225–692 fg) per pg of lens membrane protein. In aged lenses, the amount of pSer235 peaked at an average normalized lens distance of 0.89 (range = 0.89–0.90), as seen in Fig. 3 and Supplemental Fig. 4b. At this distance, the average absolute amount of pSer235 was 554 fg (range = 393–720 fg) per pg of lens membrane protein. Similar to MP20, a noticeable decrease in the amount of pSer235 occurred in aged lenses soon after it peaked, but not in young lenses. The amount of pSer235 was significantly greater in young lenses than in aged lenses starting at a normalized lens distance of 0.71 and remained as such to the lens core (Fig. 3 and Supplemental Fig. 4b). As seen for MP20, the amount of pSer235 AQP0, after peaking, remained constant across lens regions in young lenses.

Phosphorylation at AQP0 Ser229 contributed a minor amount to the total phosphorylation of AQP0, as suggested by a previous study (Ball et al., 2004). Fig. 4 and Supplemental Fig. 4c show that in young lenses, the amount of pSer229 remained at a fairly steady level in both young and old lenses. The average amount of pSer229 peaked at a normalized lens distance of 0.57 (range of 0.22–0.81), where it was 0.3 fg (range = 0.2–0.3 fg) per pg of lens membrane protein. In aged lenses, phosphorylation at this site peaked at an average normalized lens distance of 0.78 (range = 0.76–0.80), as seen in Fig. 4 and Supplemental Fig. 4c. At this distance, the average absolute amount pSer229 was 0.4 fg (range = 0.2–0.6 fg) per pg of lens membrane protein. The amount of pSer229 was not significantly different in young lenses compared to aged lenses The shallow decrease in phosphorylation at pSer229 in aged lenses minimizes the differences in phosphorylation at this site between young and aged lenses, in contrast to phosphorylation at AQP0 pSer235 and MP20 pSer170.

3.4. Pre- and post-permeability barrier changes in phosphorylation

The maximum and minimum absolute amounts of phosphorylation were determined, respectively, for each lens in regions defined as pre- and post-permeability barrier – a region described by Moffat et al. (1999) and Sweeney and Truscott (1998) as being located at the interface between the nucleus and cortex or at a distance of 7.2 mm, respectively. In this

study an r/a ratio of 0.78 represents the barrier distance based on average measurements for the adult nucleus (7 mm) and the diameter of human lenses (9 mm) (Garland et al., 1996). Therefore based on the curves for younger and older lenses, the pre-barrier region includes a normalized lens distance range of 0.99–0.78 in young lenses and 0.97–0.78 in aged lenses. The post-barrier region includes a normalized lens distance range of 0.77–0.22 in young lenses and 0.77–0.11 in aged lenses. As seen in Fig. 5, panel A, the average pre-barrier maximum amount of phosphorylation in young lenses was not significantly different from the average post-barrier minimum amount of phosphorylation for AQP0 pSer235 or AQP0 pS229, although there was a trend toward lower AQP0 pSer235 levels post-barrier. The difference in pre- and post-barrier levels in young lenses (panel A) was significantly different for MP20 pSer170 ($p = 0.03$), where it dropped approximately 4 fold. In aged lenses (Fig. 5, panel B) the average pre-barrier maximum amount of phosphorylation was significantly higher than the average post-barrier minimum amount of phosphorylation for AQP0 pSer235 ($p = 0.01$), MP20 pSer170 ($p = 0.02$), and AQP0 pSer229 ($p = 0.04$). AQP0 pSer235 and MP20 pSer170 dropped approximately 30 fold and 50 fold respectively, while AQP0 pSer229 only dropped approximately 2 fold.

Fig. 5 also highlights the quantitative differences in phosphorylation for these three peptides. In the pre-barrier region, the absolute amount of APQ0 pSer235 is roughly 100 fold higher than the absolute amount of MP20 pSer170 and 1000 fold higher than the absolute amount of AQP0 pSer229. These differences appear in the pre-barrier regions of both young (panel A) and old (panel B) lenses. In the post-barrier region of aged lenses (panel B), the absolute amount of AQP0 pSer235 changes to roughly 200 fold and 50 fold higher than the absolute amount of MP20 pSer170 and AQP0 pSer229, respectively. Thus, the phosphorylation level of AQP0 pSer235 is decreased more substantially than that of MP20 pSer170 and AQP0 pSer229 in the post-barrier region of older lenses.

4. Discussion

In the lens, PTMs are means of altering protein function in fiber cells that no longer synthesize proteins (Gonen et al., 2004a; Grey et al., 2009; Lin et al., 1998). Therefore, determining the spatial distributions of PTMs across the lens is important for understanding how the effects of PTMs on protein function influence overall lens function and transparency. In the present work, the distributions of phosphorylated AQP0 and MP20 were determined from the lens periphery to the lens center via absolute quantitation in carefully dissected samples, permitting a correlation between the changes in these distributions and molecular and physiological changes in the lens.

The distribution of MP20 pSer170 throughout the lens had not been previously studied and was determined here in human lenses. In aged lenses, MP20 pSer170 peaks at a normalized lens distance of 0.91, which correlates with the formation of a barrier to extracellular diffusion in aged human lenses (Lim et al., 2009). However, MP20 pSer170 also peaks at a normalized lens distance of 0.90 in younger lenses. While it has been suggested that MP20 plays an important role in fiber cell adhesion, the effect of phosphorylation on its function and/or distribution is unknown. Other proteins from the large claudin superfamily of which MP20 is a part affect the permeability of tight junctions upon phosphorylation (D'Souza et

al., 2007, 2005; Van Itallie and Anderson, 2006), suggesting that an increase in MP20 phosphorylation could affect fiber-to-fiber adhesion and play a role in the formation of a barrier to extracellular diffusion that is observed in aged human lenses. Since the amount of MP20 pSer 170 peaks near the permeability barrier in both young and aged lenses and is not significantly different with age (4.1 and 3.0 fg/pg lens membrane protein, respectively), it seems unlikely that phosphorylation at this site is responsible for the permeability barrier.

The amount of MP20 pSer170 declines rapidly after a normalized lens distance of 0.81 in the aged lenses, while it remains at higher levels in young lenses. At this distance, it is possible (due to species differences) that the loss of phosphorylation is due to protein phosphatase 1 (PP1), which is present mainly in the peripheral fiber cells of bovine and rat lenses (Li et al., 2001). Alternatively, the loss of signal for pSer170 may indicate that the C-terminus of MP20 is further modified with increasing lens age. One possibility is further phosphorylation of the C-terminus at Thr171. Although diphosphorylated MP20 (pSer170/pThr171) was not detected in these human lenses, potentially due to poor interaction with the HPLC stationary phase, it is present at approximately 14% in bovine lenses (Ervin et al., 2005).

An age-related decline in phosphorylation is also observed for AQP0 pSer235. While the maximum amount of pSer235 remains fairly high in young lenses, the amount of pSer235 declines significantly in aged lenses after a normalized lens distance of 0.71, likely altering AQP0 water permeability in aged fiber cells. Phosphorylation of AQP0 C-terminal peptides reduces their affinity to Ca^{2+}-CaM (Gold et al., 2012; Reichow and Gonen, 2008; Rose et al., 2008), and, at the intact protein level, promotes a high water permeability state for AQP0 (Németh-Cahalan et al., 2004; Németh-Cahalan and Hall, 2000; Varadaraj et al., 2005). Water permeability of oocytes expressing the phosphomimetic AQP0 Ser235Asp increases in high Ca^{2+} conditions (Kalman et al., 2008), reinforcing the findings of AQP0 permeability experiments conducted with lens vesicles (Varadaraj et al., 2005). Modeling of the AQP0-Ca^{2+}-CaM interaction (Reichow et al., 2013; Reichow and Gonen, 2008) and water permeability studies of AQP0 phosphomimetics in oocytes (Kalman et al., 2008) support a low water permeability state for AQP0 in the presence of Ca^{2+}-CaM. Therefore, the measurement of AQP0 Ser235 phosphorylation is critically important to understanding water permeability across the entire lens and how it fits into the lens circulation model (Mathias et al., 2007). The loss of AQP0 pSer235, which becomes statistically significant at a normalized lens distance of 0.71 in aged lenses, would be expected to permit Ca^{2+}-CaM binding and limit AQP0 water permeability. Indeed, the region where AQP0 pSer235 begins decreasing in aged lenses corresponds with the region where a barrier to water and GSH transport forms in aged human lenses (Moffat et al., 1999; Sweeney and Truscott, 1998), suggesting that the decrease in AQP0 pSer235 may be a contributing factor to barrier formation. A model, based on the one presented in (Kalman et al., 2008) and incorporating the data reported both previously (Gold et al., 2012; Reichow and Gonen, 2008; Rose et al., 2008) and here is presented in Fig. 6 to illustrate this point.

The distribution of AQP0 pSer229 was also mapped. Phosphorylation at this site did not decline rapidly towards the lens center, as it did for pSer235, but was maintained across the young lenses and only decreased slightly in the aged lenses. The absolute amount of

phosphorylation at this site was roughly 1000 fold lower than the absolute amount of phosphorylation at AQP0 Ser235, except in the post-barrier region of aged lenses, where it was only 50 fold lower. It is possible that AQP0 pSer229, which also appears to inhibit CaM binding (Kalman et al., 2008) may maintain a high water permeability state for a small number of AQP0 channels.

5. Conclusions

The quantitative analysis of AQP0 and MP20 phosphorylation presented here reveals the locations within human lenses where phosphorylation is maximum and how the distributions change with age, contributing to a growing understanding of the regulation of lens membrane proteins. AQP0 water transport is important to internal lens circulation (Mathias et al., 2007), and its regulation may affect the delivery of nutrients and antioxidants to deeper lying fiber cells. Understanding the factors that affect AQP0 water permeability, such as phosphorylation, Ca^{2+} concentration, and pH level, and their distributions in the lens is important to determine 1) if regulation is altered with age, 2) if altered regulation may contribute to cataract formation, and 3) if water permeability can be restored to prevent/relieve cataract formation.

Supplementary Material

Refer to Web version on PubMed Central for supplementary material.

Acknowledgments

The authors acknowledge funding from NIH EY-13462 and support from the Vanderbilt Vision Research Center (P30 EY-08126). They also acknowledge the use of the mass spectrometry facility at Vanderbilt University (NIH EY013462) and the Medical University of South Carolina. The authors would like to acknowledge Glenn A. Miller for statistical guidance.

Abbreviations

AQ	absolute quantity
AQP0	aquaporin 0
AQUA	absolute quantification
AUC	area under the curve
END	endogenous
IS	internal standard
m/z	mass to charge ratio
PTM	post-translational modification
r/a	normalized lens distance
Ser	serine

Thr	threonine
XIC	extracted ion chromatogram

References

Al-Ghoul KJ, Kirk T, Kuszak AJ, Zoltoski RK, Shiels A, Kuszak JR. Lens structure in MIP-deficient mice. Anat Rec A Discov Mol Cell Evol Biol. 2003; 273:714–730. http://dx.doi.org/10.1002/ar.a.10080. [PubMed: 12845708]

Ball LE, Garland DL, Crouch RK, Schey KL. Post-translational modifications of aquaporin 0 (AQP0) in the normal human lens: spatial and temporal occurrence. Biochemistry. 2004; 43:9856–9865. http://dx.doi.org/10.1021/bi0496034. [PubMed: 15274640]

Bassnett S. Lens organelle degradation. Exp Eye Res. 2002; 74:1–6. http://dx.doi.org/10.1006/exer.2001.1111. [PubMed: 11878813]

Broekhuyse RM, Kuhlmann ED, Stols AL. Lens membranes II. Isolation and characterization of the main intrinsic polypeptide (MIP) of bovine lens fiber membranes. Exp Eye Res. 1976; 23:365–371. [PubMed: 976377]

Brönstrup M. Absolute quantification strategies in proteomics based on mass spectrometry. Expert Rev Proteomics. 2004; 1:503–512. http://dx.doi.org/10.1586/14789450.1.4.503. [PubMed: 15966845]

Chandy G, Zampighi GA, Kreman M, Hall JE. Comparison of the water transporting properties of MIP and AQP1. J Membr Biol. 1997; 159:29–39. [PubMed: 9309208]

Donaldson P, Kistler J, Mathias RT. Molecular solutions to mammalian lens transparency. News Physiol Sci. 2001; 16:118–123. [PubMed: 11443230]

Donaldson PJ, Grey AC, Merriman-Smith BR, Sisley AMG, Soeller C, Cannell MB, Jacobs MD. Functional imaging: new views on lens structure and function. Clin Exp Pharmacol Physiol. 2004; 31:890–895. http://dx.doi.org/10.1111/j.1440-1681.2004.04099.x. [PubMed: 15659055]

D'Souza T, Agarwal R, Morin PJ. Phosphorylation of claudin-3 at threonine 192 by cAMP-dependent protein kinase regulates tight junction barrier function in ovarian cancer cells. J Biol Chem. 2005; 280:26233–26240. http://dx.doi.org/10.1074/jbc.M502003200. [PubMed: 15905176]

D'Souza T, Indig FE, Morin PJ. Phosphorylation of claudin-4 by PKCepsilon regulates tight junction barrier function in ovarian cancer cells. Exp Cell Res. 2007; 313:3364–3375. http://dx.doi.org/10.1016/j.yexcr.2007.06.026. [PubMed: 17678893]

Ervin LA, Ball LE, Crouch RK, Schey KL. Phosphorylation and glycosylation of bovine lens MP20. Invest Ophthalmol Vis Sci. 2005; 46:627–635. http://dx.doi.org/10.1167/iovs.04-0894. [PubMed: 15671292]

Faulkner-Jones B, Zandy AJ, Bassnett S. RNA stability in terminally differentiating fibre cells of the ocular lens. Exp Eye Res. 2003; 77:463–476. [PubMed: 12957145]

Gao J, Sun X, Martinez-Wittinghan FJ, Gong X, White TW, Mathias RT. Connections between connexins, calcium, and cataracts in the lens. J Gen Physiol. 2004; 124:289–300. http://dx.doi.org/10.1085/jgp.200409121. [PubMed: 15452195]

Garland DL, Duglas-Tabor Y, Jimenez-Asensio J, Datiles MB, Magno B. The nucleus of the human lens: demonstration of a highly characteristic protein pattern by two-dimensional electrophoresis and introduction of a new method of lens dissection. Exp Eye Res. 1996; 62:285–291. http://dx.doi.org/10.1006/exer.1996.0034. [PubMed: 8690038]

Gerber SA, Rush J, Stemman O, Kirschner MW, Gygi SP. Absolute quantification of proteins and phosphoproteins from cell lysates by tandem MS. Proc Natl Acad Sci USA. 2003; 100:6940–6945. http://dx.doi.org/10.1073/pnas.0832254100. [PubMed: 12771378]

Gold MG, Reichow SL, O'Neill SE, Weisbrod CR, Langeberg LK, Bruce JE, Gonen T, Scott JD. AKAP2 anchors PKA with aquaporin-0 to support ocular lens transparency. EMBO Mol Med. 2012; 4:15–26. http://dx.doi.org/10.1002/emmm.201100184. [PubMed: 22095752]

Golestaneh N, Fan J, Zelenka P, Chepelinsky AB. PKC putative phosphorylation site Ser235 is required for MIP/AQP0 translocation to the plasma membrane. Mol Vis. 2008; 14:1006–1014. [PubMed: 18523655]

Gonen T, Cheng Y, Kistler J, Walz T. Aquaporin-0 membrane junctions form upon proteolytic cleavage. J Mol Biol. 2004a; 342:1337–1345. http://dx.doi.org/10.1016/j.jmb.2004.07.076. [PubMed: 15351655]

Gonen T, Sliz P, Kistler J, Cheng Y, Walz T. Aquaporin-0 membrane junctions reveal the structure of a closed water pore. Nature. 2004b; 429:193–197. http://dx.doi.org/10.1038/nature02503. [PubMed: 15141214]

Grey AC, Jacobs MD, Gonen T, Kistler J, Donaldson PJ. Insertion of MP20 into lens fibre cell plasma membranes correlates with the formation of an extracellular diffusion barrier. Exp Eye Res. 2003; 77:567–574. [PubMed: 14550398]

Grey AC, Li L, Jacobs MD, Schey KL, Donaldson PJ. Differentiation-dependent modification and subcellular distribution of aquaporin-0 suggests multiple functional roles in the rat lens. Differentiation. 2009; 77:70–83. http://dx.doi.org/10.1016/j.diff.2008.09.003. [PubMed: 19281766]

Jacobs MD, Soeller C, Sisley AMG, Cannell MB, Donaldson PJ. Gap junction processing and redistribution revealed by quantitative optical measurements of connexin46 epitopes in the lens. Invest Ophthalmol Vis Sci. 2004; 45:191–199. [PubMed: 14691173]

Kalman K, Nemeth-Cahalan KL, Froger A, Hall JE. Phosphorylation determines the calmodulin-mediated Ca2+ response and water permeability of AQP0. J Biol Chem. 2008; 283:21278–21283. http://dx.doi.org/10.1074/jbc.M801740200. [PubMed: 18508773]

Kumari, SS., Eswaramoorthy, S., Mathias, RT., Varadaraj, K. Unique and analogous functions of aquaporin 0 for fiber cell architecture and ocular lens transparency. Biochim Biophys Acta. 2011. http://dx.doi.org/10.1016/j.bbadis.2011.04.001

Li DW, Xiang H, Fass U, Zhang XY. Analysis of expression patterns of protein phosphatase-1 and phosphatase-2A in rat and bovine lenses. Invest Ophthalmol Vis Sci. 2001; 42:2603–2609. [PubMed: 11581206]

Lim JC, Walker KL, Sherwin T, Schey KL, Donaldson PJ. Confocal microscopy reveals zones of membrane remodeling in the outer cortex of the human lens. Invest Ophthalmol Vis Sci. 2009; 50:4304–4310. http://dx.doi.org/10.1167/iovs.09-3435. [PubMed: 19357350]

Lin JS, Eckert R, Kistler J, Donaldson P. Spatial differences in gap junction gating in the lens are a consequence of connexin cleavage. Eur J Cell Biol. 1998; 76:246–250. [PubMed: 9765054]

Louis CF, Johnson R, Johnson K, Turnquist J. Characterization of the bovine lens plasma membrane substrates for cAMP-dependent protein kinase. Eur J Biochem. 1985; 150:279–286. http://dx.doi.org/10.1111/j.1432-1033.1985.tb09018.x. [PubMed: 2990930]

Louis CF, Hur KC, Galvan AC, TenBroek EM, Jarvis LJ, Eccleston ED, Howard JB. Identification of an 18,000-dalton protein in mammalian lens fiber cell membranes. J Biol Chem. 1989; 264:19967–19973. [PubMed: 2584203]

Mathias RT, Rae JL, Baldo GJ. Physiological properties of the normal lens. Physiol Rev. 1997; 77:21–50. [PubMed: 9016299]

Mathias RT, Kistler J, Donaldson P. The lens circulation. J Membr Biol. 2007; 216:1–16. http://dx.doi.org/10.1007/s00232-007-9019-y. [PubMed: 17568975]

Moffat BA, Landman KA, Truscott RJ, Sweeney MH, Pope JM. Age-related changes in the kinetics of water transport in normal human lenses. Exp Eye Res. 1999; 69:663–669. http://dx.doi.org/10.1006/exer.1999.0747. [PubMed: 10620395]

Németh-Cahalan KL, Hall JE. pH and calcium regulate the water permeability of aquaporin 0. J Biol Chem. 2000; 275:6777–6782. [PubMed: 10702234]

Németh-Cahalan KL, Kalman K, Hall JE. Molecular basis of pH and Ca2+ regulation of aquaporin water permeability. J Gen Physiol. 2004; 123:573–580. http://dx.doi.org/10.1085/jgp.200308990. [PubMed: 15078916]

Reichow SL, Gonen T. Noncanonical binding of calmodulin to aquaporin-0: implications for channel regulation. Structure. 2008; 16:1389–1398. http://dx.doi.org/10.1016/j.str.2008.06.011. [PubMed: 18786401]

Reichow SL, Clemens DM, Freites JA, Németh-Cahalan KL, Heyden M, Tobias DJ, Hall JE, Gonen T. Allosteric mechanism of water channel gating by Ca2+–calmodulin. Nat Struct Mol Biol. 2013; 20:1085–1092. http://dx.doi.org/10.1038/nsmb.2630. [PubMed: 23893133]

Lindsey Rose KM, Gourdie RG, Prescott AR, Quinlan RA, Crouch RK, Schey KL. The C terminus of lens aquaporin 0 interacts with the cytoskeletal proteins filensin and CP49. Invest Ophthalmol Vis Sci. 2006; 47:1562–1570. http://dx.doi.org/10.1167/iovs.05-1313. [PubMed: 16565393]

Rose KML, Wang Z, Magrath GN, Hazard ES, Hildebrandt JD, Schey KL. Aquaporin 0-calmodulin interaction and the effect of aquaporin 0 phosphorylation. Biochemistry. 2008; 47:339–347. http://dx.doi.org/10.1021/bi701980t. [PubMed: 18081321]

Schey KL, Little M, Fowler JG, Crouch RK. Characterization of human lens major intrinsic protein structure. Invest Ophthalmol Vis Sci. 2000; 41:175–182. [PubMed: 10634618]

Shiels A, Mackay D, Bassnett S, Al-Ghoul K, Kuszak J. Disruption of lens fiber cell architecture in mice expressing a chimeric AQP0-LTR protein. Faseb J. 2000; 14:2207–2212. http://dx.doi.org/10.1096/fj.99-1071com. [PubMed: 11053241]

Shiels A, King JM, Mackay DS, Bassnett S. Refractive defects and cataracts in mice lacking lens intrinsic membrane protein-2. Invest Ophthalmol Vis Sci. 2007; 48:500–508. http://dx.doi.org/10.1167/iovs.06-0947. [PubMed: 17251442]

Sweeney MH, Truscott RJ. An impediment to glutathione diffusion in older normal human lenses: a possible precondition for nuclear cataract. Exp Eye Res. 1998; 67:587–595. http://dx.doi.org/10.1006/exer.1998.0549. [PubMed: 9878221]

Van Itallie CM, Anderson JM. Claudins and epithelial paracellular transport. Annu Rev Physiol. 2006; 68:403–429. http://dx.doi.org/10.1146/annurev.physiol.68.040104.131404. [PubMed: 16460278]

Varadaraj K, Kushmerick C, Baldo GJ, Bassnett S, Shiels A, Mathias RT. The role of MIP in lens fiber cell membrane transport. J Membr Biol. 1999; 170:191–203. [PubMed: 10441663]

Varadaraj K, Kumari S, Shiels A, Mathias RT. Regulation of aquaporin water permeability in the lens. Invest Ophthalmol Vis Sci. 2005; 46:1393–1402. http://dx.doi.org/10.1167/iovs.04-1217. [PubMed: 15790907]

Wang Z, Han J, David LL, Schey KL. Proteomics and phosphoproteomics analysis of human lens fiber cell membranes. Invest Ophthalmol Vis Sci. 2013; 54:1135–1143. http://dx.doi.org/10.1167/iovs.12-11168. [PubMed: 23349431]

Wilson JLL, Miranda CA, Knepper MA. Vasopressin and the regulation of aquaporin-2. Clin Exp Nephrol. 2013; 17:751–764. http://dx.doi.org/10.1007/s10157-013-0789-5. [PubMed: 23584881]

Appendix A. Supplementary data

Supplementary data related to this article can be found at http://dx.doi.org/10.1016/j.exer.2016.06.015.

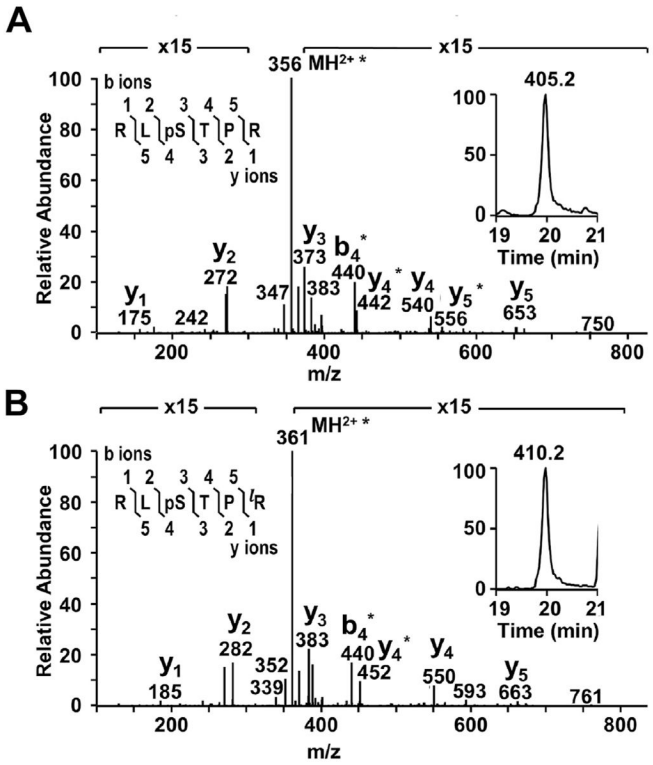

Fig. 1.

Identification and quantitation of MP20 168–173 pSer170. MS/MS spectra from an 18 year old lens confirmed the identity of A) endogenous MP20 168–173 pSer170 and B) its isotopically labeled AQUA peptide internal standard. Within the MS/MS spectra, the asterisks represent loss of phosphoric acid. The peptide sequence and fragmentation are shown in the top left corner of each panel, where phosphorylation is indicated by "p" and the isotopically labeled amino acid is indicated by "***l***" (bottom panel only). The XICs of MP20 168–173 pSer170 (panel A, insert) and its AQUA internal standard (panel B, insert) show the difference in mass between the $(M+2H)^{2+}$ ions for the endogenous and labeled peptides and the identical elution times of these peptides.

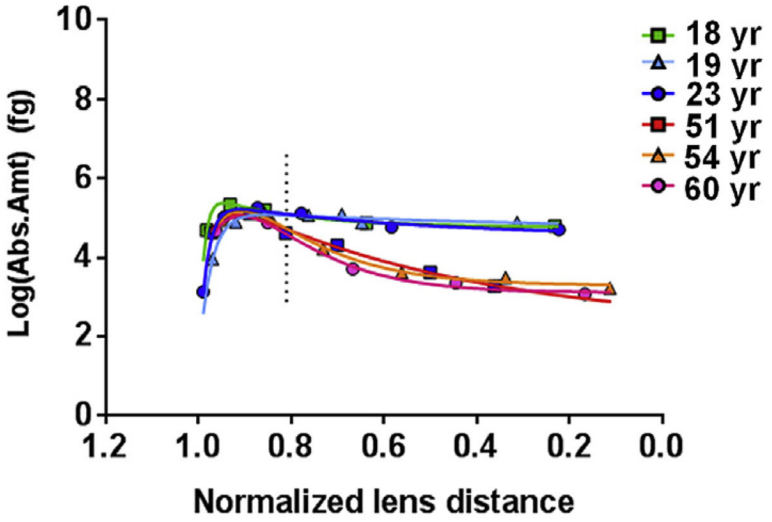

Fig. 2.

Distribution of MP20 Ser170 phosphorylation in various aged lenses. MP20 pSer170 is differentially distributed across the lens and becomes significantly lower in older lenses at a normalized lens distance of 0.81 ($p = 0.02$; vertical dotted line), remaining as such to the lens center. The value graphed here represents the amount of phosphorylated peptide measured per sample. The amount of phosphorylated peptide per picogram of lens membrane protein (as stated in the text) can be determined by dividing this value by 42,183 pg. R^2 values for the curves are as follows, 18 yr–0.99, 19 yr–0.97, 23 yr–0.99, 51 yr–0.99, 54 yr–0.99, 60 yr–0.99. Error bars represent standard deviation. See Supplemental Fig. 4a for the 95% confidence bands of the curves.

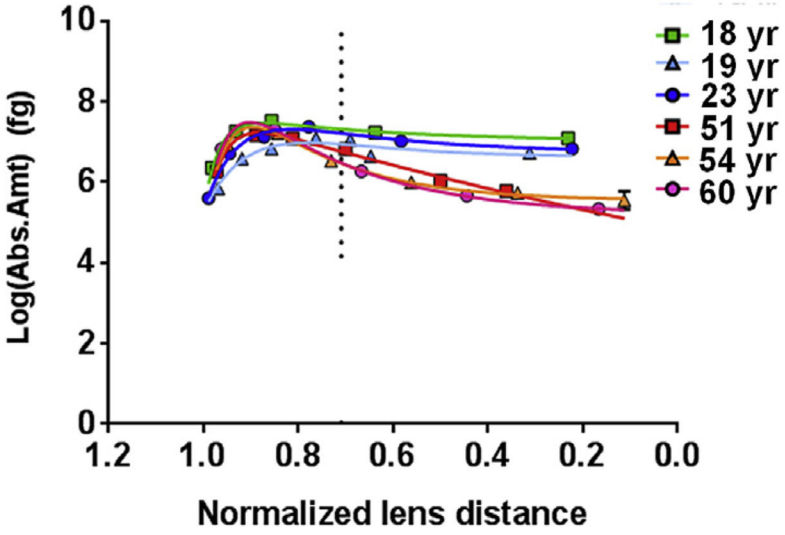

Fig. 3.

Distribution of AQP0 Ser235 phosphorylation in various aged lenses. AQP0 pSer235 is differentially distributed, across the lens and becomes significantly lower in older lenses at a normalized lens distance of 0.71 ($p = 0.04$; vertical dotted line), remaining as such to the lens center. The value graphed here represents the amount of phosphorylated peptide measured per sample. The amount of phosphorylated peptide per picogram of lens membrane protein (as stated in the text) can be determined by dividing this value by 42,183 pg. R^2 values for the curves are as follows, 18 yr–0.99, 19 yr–0.91, 23 yr–0.99, 51 yr–0.99, 54 yr–1.00, 60 yr–1.00. Error bars represent standard deviation. See Supplemental Fig. 4b for the 95% confidence bands of the curves.

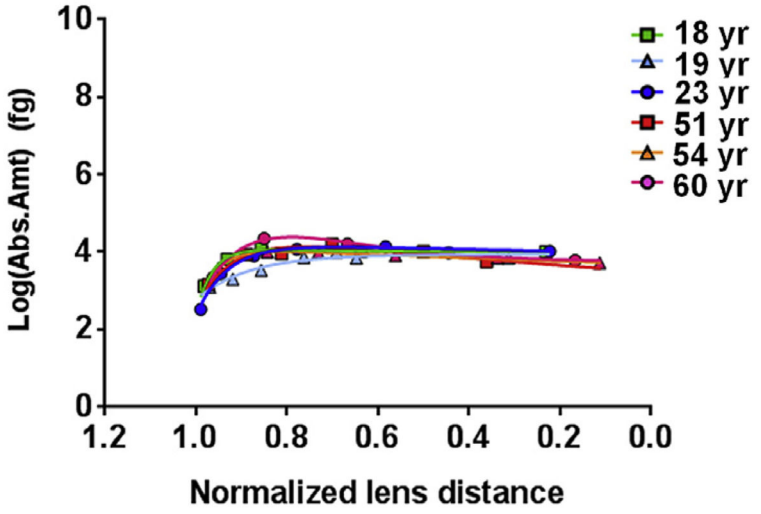

Fig. 4.

Distribution of AQP0 Ser229 phosphorylation in various aged lenses. The average amount of AQP0 pS229 in young and aged lenses is not significantly different. The value graphed here represents the amount of phosphorylated peptide measured per sample. The amount of phosphorylated peptide per picogram of lens membrane protein (as stated in the text) can be determined by dividing this value by 42,183 pg. R^2 values for the curves are as follows, 18 yr–0.99, 19 yr–0.93, 23 yr–0.99, 51 yr–0.93, 54 yr–1.00, 60 yr–0.99. Error bars represent standard deviation. See Supplemental Fig. 4c for the 95% confidence bands of the curves.

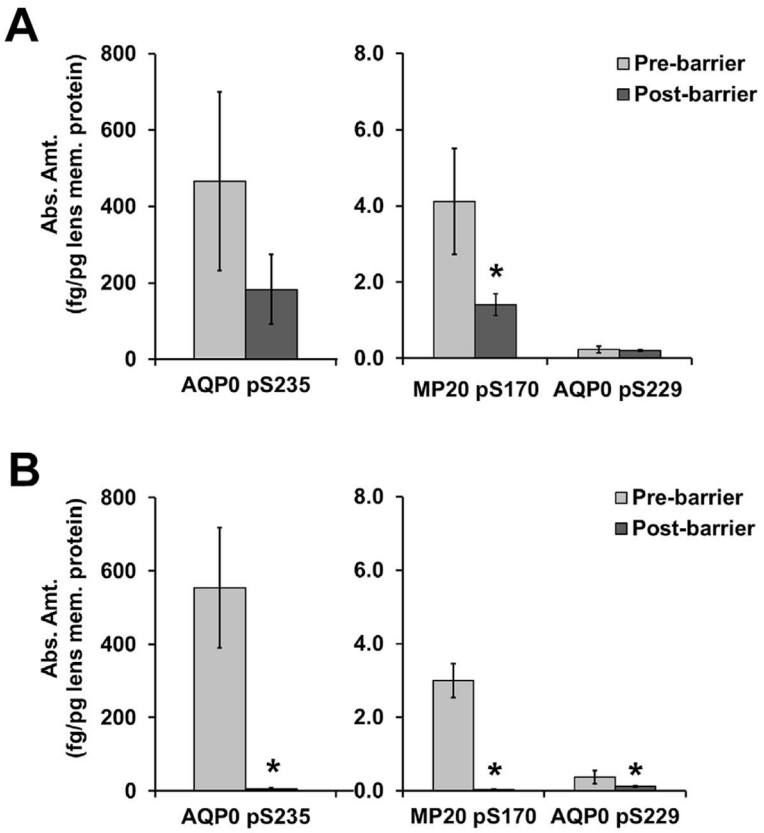

Fig. 5.

Comparison of phosphorylation relative to the permeability barrier. The maximum amount of phosphorylation pre-barrier and the minimum amount of phosphorylation post-barrier are shown for three peptides in both A) young and B) aged lenses. The asterisks represent a statistically significant ($p < 0.05$) difference between pre- and post-barrier amounts of phosphopeptide.

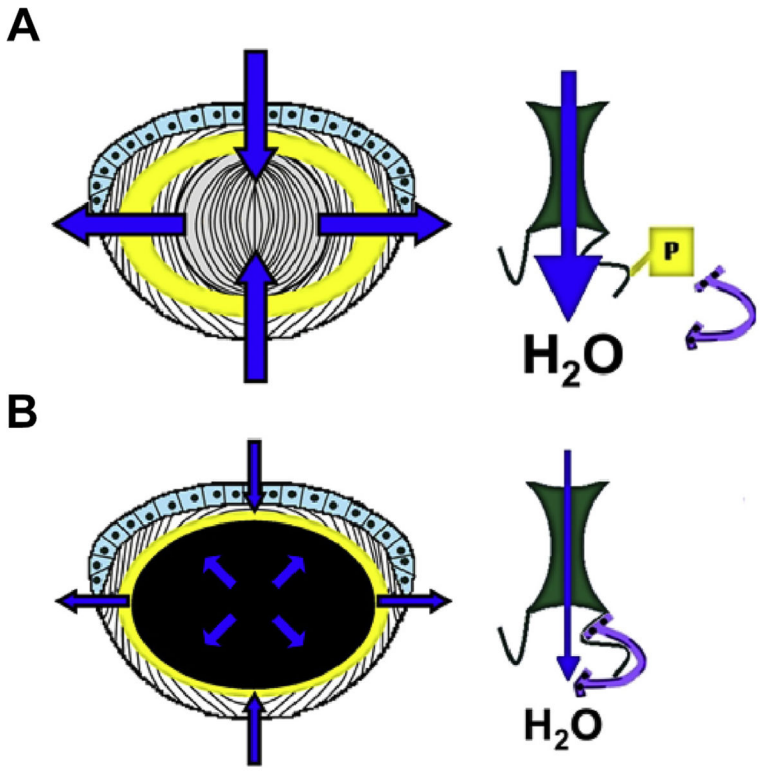

Fig. 6.

Potential effects of the differential distribution of AQP0 Ser235 phosphorylation. This model, based on Kalman et al., 2008, incorporates the present findings with data regarding the effect of phosphorylation on AQP0-Ca^{2+}-CaM binding (Gold et al., 2012; Reichow and Gonen, 2008; Rose et al., 2008) and the effect of Ca^{2+}-CaM on AQP0 water permeability (Kalman et al., 2008; Reichow and Gonen, 2008). A) In young lenses, phosphorylation of AQP0 Ser235 peaks at an average normalized lens distance of 0.82 (represented by the yellow shaded region (left) and remains fairly high, suggesting that young lenses will have efficient water flow throughout the lens, as indicated by the broad blue arrows. B) In aged lenses, phosphorylation of AQP0 Ser235 decreases significantly starting at a normalized lens distance of 0.71 (represented by the black shaded region, left), permitting Ca^{2+}-CaM binding (purple horseshoe shape, right) and decreasing AQP0 water permeability, as indicated by the narrow blue arrows. This may play a role in the formation of a barrier to water transport in aged lenses. The design of the lens cartoon (panels A and B, left side) was derived from (Donaldson et al., 2001). Note, this is a cartoon and is meant to illustrate the described concept not specific molecular interactions.

Table 1

AQUA internal standard phosphopeptide

Peptide	Sequence[a]
AQP0 229–238 pSer235	SISE^{l}RLpSVLK
AQP0 227–233 pSer231	LKSIpSE^{l}R
MP20 168–173 pSer170	RLpSTP^{l}R

[a]Isotopically labeled arginines (^{13}C6·^{15}N4) are designated by "***l***", and "p" indicates a phosphorylated residue.